Langmuir
Article
pubs.acs.org/Langmuir

Two Liquids Wetting and Low Hysteresis Electrowetting on Dielectric Applications

Mathieu Maillard,* Julien Legrand, and Bruno Berge

Varioptic, 24b rue Jean Baldassini, 69007 Lyon, France

Received December 15, 2008. Revised Manuscript Received February 16, 2009

This study focuses on electrowetting using two immmiscible liquids on a dielectric coating. It is demonstrated that low contact angle of oil on the hydrophobic surfaces is a key parameter to obtain a low hysteresis system, below 2°. On the basis of these results, three aspects of the wetting properties have been studied: the influence of the surface hydrophobic properties, the design of the liquids according to the hydrophobic surface, and a graphical method to solve the Bartell-Osterhof equation and predict the wetting properties of two liquids on a surface. These results define clear design rules to obtain a low hysteresis system, useful for many applications from liquid lenses to displays and laboratory-on-a-chip.

Introduction

Electrowetting on dielectric is now a widely studied phenomenon for numerous applications since this field was reintroduced in the late 1980s by several groups in the field of electro-optics applications[1] using mercury droplets and later by Berge[2] using water-based systems, a century after early work from Lippmann.[3] Several industrial applications are being developed and commercialized[4] like liquid lens,[5] displays,[6] or liquid displacement for laboratory-on-a-chip biological applications.[7,8] It has also been an intense research field,[9] from the theoretical point of view, e.g., in interface tension and interfacial potential, and many questions arose after preliminary work, e.g., the origin of the electrowetting saturation occurring at high electric field[10] and hysteresis.

In the case of a drop of nonconducting liquid, standing on an insulating layer, surrounded by a conducting liquid, the electrowetting phenomenon is fairly well described by the following equation:

$$\cos\theta_{OW} = \cos\theta^0_{OW} - \frac{\varepsilon\varepsilon_0}{2d\gamma} {V_{RMS}}^2 \qquad (1)$$

with θ_{OW} the natural contact angle (as measured without applied voltage), ε the dielectric constant of the dielectric layer, ε_0 the permittivity of vacuum, d the dielectric thickness, γ the interface tension, and V_{rms} the rms value of the applied voltage. As described by this equation, the contact angle from the nonconducting droplet is thus increasing with applied voltage. This equation remains valid as long as voltage does not exceed the saturation voltage.

In a liquid lens, the oil droplet acts as a lens with a variable focal length depending on the contact angle and the applied voltage. As a consequence, the device hysteresis also depends on the electrowetting hysteresis. In an optical device like a liquid lens, hysteresis is a limiting factor for an accurate focus, because it induces an uncertainty into the focusing precision. In other applications like MEMS, hysteresis is also a limitation to moving droplets because it increases the actuation voltage.

For these reasons, it is a key parameter for many applications to determine ways to reduce it as low as possible, as it is a limitation for an accurate and reproducible actuation.

Experimental Setup

In the present work, electrowetting experiments are performed using two liquids, one being a polar conducting liquid and the other one replacing the air, being an insulating nonpolar liquid, like a mineral or silicone oil. The insulating coating is a thin layer of Parylene C, between 4 and 6 μm thick, deposited by a vapor deposition process (VDP)[17] on a semipolished stainless steel plate (roughness was measured as $r_a < 0.1\,\mu$m). Voltage was applied at 1 kHz with a sine waveform, up to 70 V using a LCR meter Agilent 4284A amplified with a TEGAM 2340. Sample was insulated on the stainless steel side and immersed in the conducting fluid; a drop of oil was deposited on the hydrophobic coating, roughly 2 mm in diameter. Oil and conducting fluids used were made according to Table 1; silicon oil DC702, DC704 EU, and DC705 were purchased from Dow-Corning, phenyltris(trimethylsiloxy) silane was purchased from Gelest Inc., and the other compounds from Sigma-Aldrich without any further purification.

Table 1. Oil and Conducting Fluids Compositions, as Used in Experiments Described by Figures 1−4[a]

oil		conducting fluid	
Phenyltris(trimethylsiloxy)silane	35.00%	Water	33.30%
DC 704 EU	25.10%	Na_2SO_4	0.20%
DC 702	15.00%	1,2,3-propanetriol	22.70%
DC 705	5.00%	1,2-propanediol	43.80%
1,6-dibromohexane	19.90%		

[a] This oil has also been modified to increase the contact angle (see result in Figure 3), decreasing dibromohexane to 9.9% and increasing phenyltris(trimethylsiloxy)silane to 45%.

*Author email address: mathieu.maillard@varioptic.com.

(1) Beni, G.; Hackwood, S. *Appl. Phys. Lett.* **1981**, *38*(4), 207–209.
(2) Berge, B. *C. R. Acad. Sci. Paris* **1993**, *317*, 157.
(3) Lippmann, G. *Ann. Chim. Phys.* **1875**, *5*, 497.
(4) Shamai, R.; Andelman, D.; Berge, B.; Hayes, R. *Soft Matter* **2008**, *4*, 38.
(5) Berge, B.; Peseux, J. *Eur. Phys. J. E* **2000**, *3*, 159–163.
(6) Roques-Carmes, T.; Hayes, R. A.; Feenstra, B. J; Schlangen, L. J. M. *J. Appl. Phys.* **2004**, *95*(8), 4389–4396.
(7) Fair, R. B.; Khlystov, A.; Tailor, T. D.; Ivanov, V.; Evans, R. D.; Griffin P. B.; Vijay, S.; Pamula, V. K.; Pollack, M. G.; Zhou, J. *IEEE Des. Test Comput.* **2007**, *24*, 10–24.
(8) Gu, H.; Malloggi, F.; Vanapalli, S. A.; Mugele, F. *Appl. Phys. Lett.* **2008**, *93*, 183507.
(9) Mugele, F.; Buehrle, J. *J. Phys.: Condens. Matter* **2007**, *19*, 375112.
(10) Drygiannakis, A. I.; Papathanasiou, A. G.; Boudouvis, A. G. *J. Colloid Interface Sci.* **2008**, *326*(2), 451–459.

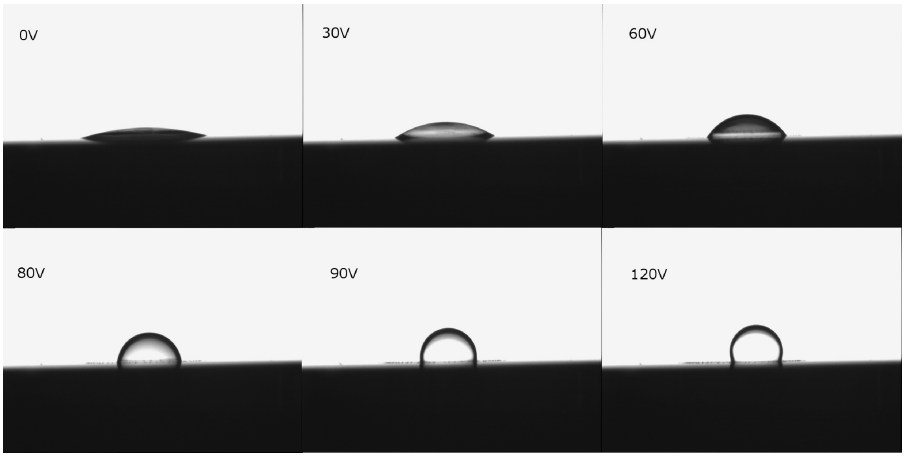

Figure 1. Image capture of an oil drop standing on a parylene coating, immersed in a conducting fluid for various applied voltages at 1 kHz from 0 to 120 V_{rms}.

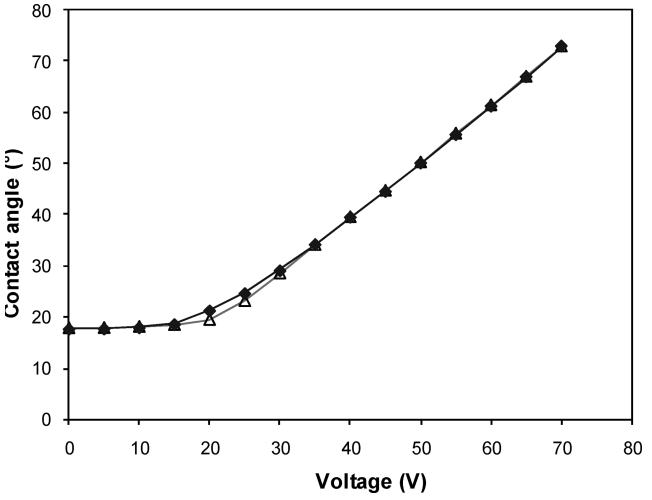

Figure 2. Advancing (diamond) and receding (triangles) contact angle from an oil drop depending on the applied voltage between 0 and 70 V. In this figure, we observe a maximum hysteresis of 1.9° at 20 V and a natural contact angle of 17°, as observed at 0 V.

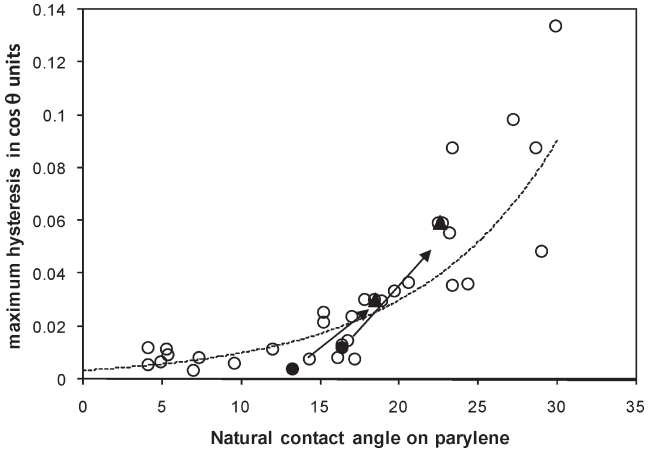

Figure 3. Maximum contact angle hysteresis measured by electrowetting depending on the natural contact angle.

Contact angle was measured using a Krüss goniometer during the voltage ramp application, i.e., typically from 0 to 70 V with 5 V steps every 2 s to allow the contact angle to reach equilibrium. Contact angle measurement accuracy has been estimated at ±1° using the circle fitting method for the low contact angle (< 30°).

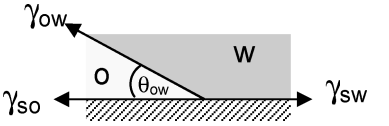

Figure 4. Young's diagram with two liquids on a hydrophobic surface; O and W refer to oil and conducting fluid, respectively.

Every sample is characterized by the maximum hysteresis measured within the voltage range.

These conditions are very similar to a liquid lens and allowed us to mimic what is actually occurring in such a device.

Results on Hysteresis

Hysteresis in electrowetting is related to a problem of spreading; as voltage increases, contact angle from the insulating fluid is increasing, its curvature radius thus decreases, and drop diameter consequently decreases. This corresponds to the receding angle usually observed on the rear side of a drop on an inclined surface[11] On the opposite, when decreasing voltage, contact angle decreases and similarly corresponds to the advancing angle. Hysteresis is then measured as the contact angle difference at a given voltage, between the voltage ramp up and down.

Contact angle hysteresis has many origins, from surface roughness to chemical surface homogeneity, and of course to liquid−surface interaction by means of contact angle.[11,12] Substrate arithmetic roughness R_A measured on our samples using a diamond stylus profilometer was lower than 100 nm. For this reason, we did not focus in the present study on the roughness variations, assuming that surface roughness was limited and on the same order of magnitude for all the substrates we used. Electrowetting experiments have been performed on various batches of parylene coating and using various liquid compositions. For every experiment, natural contact angle (i.e., the contact angle measured without applied voltage) has been measured as well as contact angle as a function of applied voltage. Figure 1 represents image capture of a typical experiment; for each voltage, the oil drop contact angle θ_{OW} on the surface immersed in conducting fluid changes according to the electrowetting equation.

A typical electrowetting curve is given in Figure 2: we obtain in the present example a hysteresis of 1.9° measured as the maximum

(11) de Gennes, P. G. *Rev. Mod. Phys.* **1985**, *57*, 3.
(12) Decker, E. L.; Garoff, S. *Langmuir* **1996**, *12*(8), 2100–2110.

difference between the receding and the advancing curve in the useful range of contact angles 0−70°. Over several experiments, we obtain hysteresis values ranging from below 2°, which is roughly our instrument precision, to up to tens of degrees, for the extreme configurations. We limited the experiment to about 70 V to avoid any saturation phenomenon and because it corresponds to the contact angle range used in the liquid lens application.

In Figure 3, maximum hysteresis has been extracted from many electrowetting experiment and is plotted depending on the natural contact angle; hollow circles correspond to various batches of parylene used with the same liquids described in Table 1. As a first observation in Figure 3, it is clear that maximum hysteresis we measured is correlated with the natural contact angle, with high contact angle inducing high hysteresis.

It was first relevant to determine if this result is purely due to a wetting variation or a roughness effect: indeed, roughness having an impact on both contact angle and hysteresis, it is possible to find a correlation between contact angle and hysteresis, not because they are directly related but because they are cross-related, through the roughness effect.

For this reason, we also performed experiments on the same batch of parylene but with liquids differing in contact angle, as described in Table 1. Each experiment is performed on exactly the same coating sample to avoid any sample variation: full circles are the original liquids, whereas the triangles are the modified ones. The arrow indicates the effect of switching from one liquid to the other, on the same substrate. Two of these experiments are presented, and each time, the change in liquids induces an increase of both the natural contact angle and hysteresis. This trend is similar to what we previously observed when measuring hysteresis on the same liquid but with hydrophobic coatings from various batches.

We also checked that this contact angle dependency was not limited to parylene and these liquids but remained true for various other substrates and formulations. As of today, we have not been able to find hydrophobic coatings and liquids that did not follow this rule.

From this, it appears clearly that:

- Maximum hysteresis is clearly related to the natural contact angle.
- It is possible to specify a maximum natural contact angle to ensure a low hysteresis system.

In the case of a liquid lens, the accuracy of the device requires a maximum hysteresis of about 0.03 in cos units, which corresponds to about 4°. According to Figure 3, this requirement is reached as long as the natural contact angle for an oil drop in a conducting liquid below 20° is obtained. This result is specifically related to the natural contact angle and thus depends on both surface and liquids: a low hysteresis is expected regardless of the surface and liquids, as long as the low natural contact angle requirement is reached.

This phenomenon is very likely related to the microscopic contact angle as studied by F. Mugele et al.[9]: on a macroscopic scale, contact angle varies with voltage according to the electrowetting relation, whereas at the close vicinity of the triple line, electric field is enhanced, inducing a large deformation of the interface. They also pointed out that the electric field component along the surface plane vanishes, leading the microscopic contact angle to match the natural contact angle, i.e., the Young's contact angle.

An alternative way to describe this phenomenon is to consider the electric field across the oil, at the vicinity of the three-phase line. As long as oil thickness is large compared to the insulating layer, electric field is negligible compared to the electric field at the conducting fluid interface and interface is modified according to the electrowetting relation. Now, if you consider the electric field at the closest vicinity of the three-phase line, as oil thickness tends to zero, electric field at the conducting fluid interface above oil and above the insulating layer tends to the same value, it is thus not surprising to consider that contact angle tends to the Young's angle at the closest vicinity of the interface, as the electric field difference tends to zero.

Now, if you consider hysteresis as a contact angle variation due to the receding and advancing displacement of the liquid interface, it seems obvious to consider that hysteresis will differ if at the microscopic scale; the slipping occurs on a surface or on a thin oil film. In the first case, hysteresis is described as a solid liquid friction phenomenon, whereas in the second case, it is limited to a liquid−liquid friction phenomenon, which is expectedly of much lower amplitude.

Hence, our experimental results are coherent with results from Mugele's work according to the fact that having a low Young's contact angle leads to a low microscopic angle even in the presence of an electric field, inducing low friction at the triple interface and thus a low hysteresis system. It has to be noted that low hysteresis is also related to the signal waveform, with hysteresis usually being much lower with ac voltage than dc voltage. This was observed experimentally and theoretically described as a microscopic vibration of the triple interface according to the voltage frequency,[13] allowing the system to overcome the friction barrier, just like any mechanical system.

Contact Angle Design. A question that arose directly from these results is how to design the liquid and hydrophobic coating in order to achieve a low contact angle system and consequently a low hysteresis system. This problem has been divided into three parts: the design of the hydrophobic surface, the nonpolar affinity of liquids on the surface, and the interfacial tension influence.

From the hydrophobic coating point of view, we carefully examined the equation giving the contact angle using two liquids on a surface to determine the most relevant parameters for a low contact angle. In the case of a two-liquid spreading as described in Figure 4, Young's equation becomes

$$\gamma_{sw} = \gamma_{so} + \gamma_{ow}.\cos\theta_{ow} \quad (2)$$

with γ_{SW}, γ_{OW}, and γ_{SO} the solid-conducting liquid, oil-conducting fluid, and solid−oil interface tensions and θ_{WO} the Young's contact angle, i.e., the natural contact angle.

Interfacial tensions between liquids and substrate can be estimated by taking into account dipolar (p) and dispersive (d) interactions using the equation from Good, Girifalco, and Fowkes[14]:

$$\gamma_{sw} = \gamma_S + \gamma_W - 2\sqrt{\gamma_S^d\gamma_W^d} - 2\sqrt{\gamma_S^p\gamma_W^p} \quad \text{for the oil} \quad (3)$$

$$\gamma_{so} = \gamma_S + \gamma_O - 2\sqrt{\gamma_S^d\gamma_O^d} - 2\sqrt{\gamma_S^p\gamma_O^p} \quad \text{for the aqueous phase} \quad (4)$$

(13) Li, F.; Mugele, F. *Appl. Phys. Lett.* **2008**, *92*, 244108.
(14) Good, R. J; Girifalco, L. A. *J. Phys. Chem.* **1960**, *64*, 561.

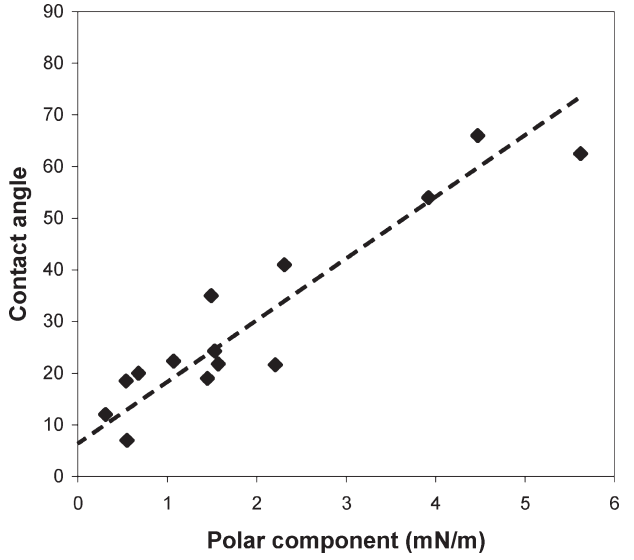

Figure 5. Contact angle from an oil drop in a conducting liquid depending on the hydrophobic coating polarity.

Table 2. Dispersive and Polar Components from the Liquids Described in Table 1

surface tension	conducting liquid	oil
γ (mN/m)	44.1	23.2
γ^p (mN/m)	25.65	2.8
γ^d (mN/m)	18.45	19.8
interface tension γ_{WO}	15 ± 1 mN/m	

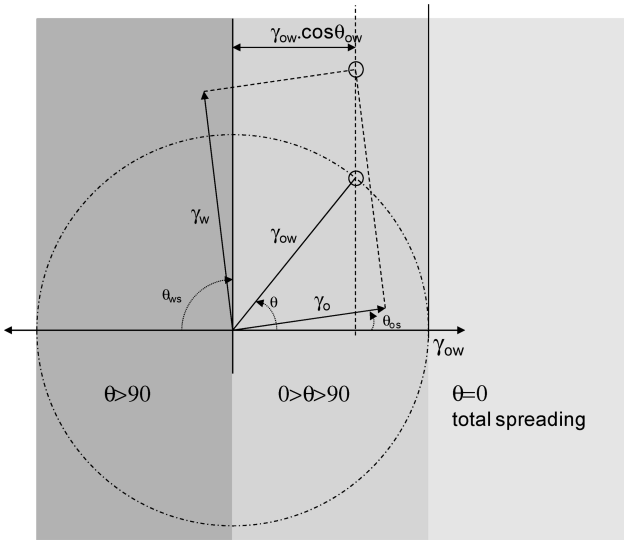

Figure 6. Graphical representation of the Bartell–Osterhof equation giving the contact angle of two liquids on a surface.

Combining eqs 2, 3, and 4, we get a relation between oil contact angle and polar and dispersive components of the surface tension

$$\gamma_{OW}\cos\theta_{OW} = \gamma_W - \gamma_O + 2\sqrt{\gamma_S^d\gamma_O^d} + 2\sqrt{\gamma_S^p\gamma_O^p} - 2\sqrt{\gamma_S^d\gamma_W^d} - 2\sqrt{\gamma_S^p\gamma_W^p} \quad (5)$$

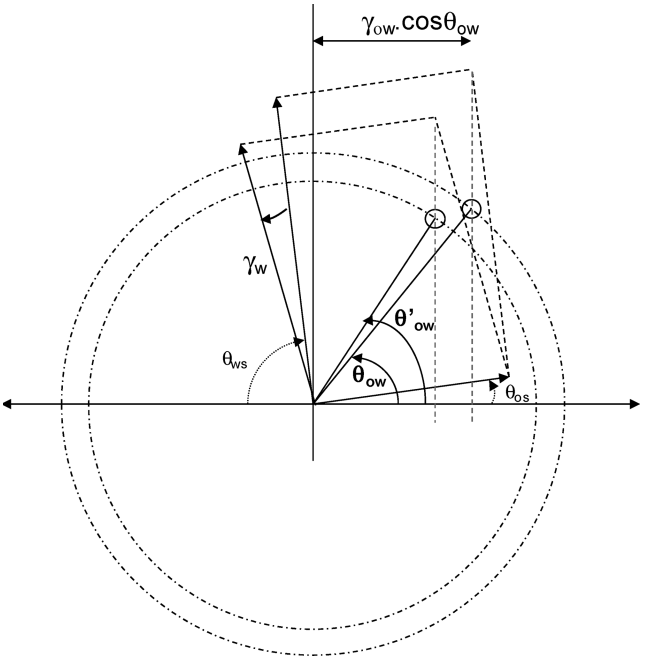

Figure 7. Graphical representation of the effect of lowering the interface tension between two liquids based on the Bartell–Osterhof equation.

Table 3. Surface Tension and Contact Angle on Parylene C and Teflon AF, in the Presence of the Conducting Fluid Described in Table 1

compound	surface tension (mN/m)	contact angle on parylene	contact angle on Teflon AF
Hexane	18.05	41.4	0
1,1,1,5,5,5-hexafluoroacetylacetone	14.74	54.5	0
pdms 2cs	18.2	57.6	9.8
heptane	20.27	37.9	0
cyclohexane	25	16.9	15.3
cyclohexylbenzène	30.62	16.8	27.6
1,10-dichlorodecane	34.54	14.7	28
1,8-dibromooctane	37.73	0	37.3
1-bromonaphtalene	43.57	0	43.1

equivalent to

$$\cos\theta_{OW} = \frac{1}{\gamma_{OW}}\left\{\gamma_W - \gamma_O + 2\sqrt{\gamma_S^d}\left(\sqrt{\gamma_O^d} - \sqrt{\gamma_W^d}\right) + 2\sqrt{\gamma_S^p}\left(\sqrt{\gamma_O^p} - \sqrt{\gamma_W^p}\right)\right\} \quad (6)$$

with $\gamma_i = \gamma_i^p + \gamma_i^d$ the surface tension in mN/m.

In the case of most commonly used liquids, dispersive components are similar $(\gamma_O^d)^{1/2} - (\gamma_W^d)^{1/2}$, whereas polar component are quite different.

Extending these equations to a two-liquid system is based on the assumption that no permanent adsorption is occurring between the liquids and the surface. This assumption is realistic, since no proteins or surfactants were used in the present system.

This large difference implies in eq 6 that contact angle will be much more sensitive to the surface polarity than its dispersive component. In other words, an increase in the surface polarity lowers the surface water interfacial tension. This effect is more important with the aqueous conducting fluid than oil, because oil is not polar, and this consequently favors the water spreading and prevents oil from spreading.

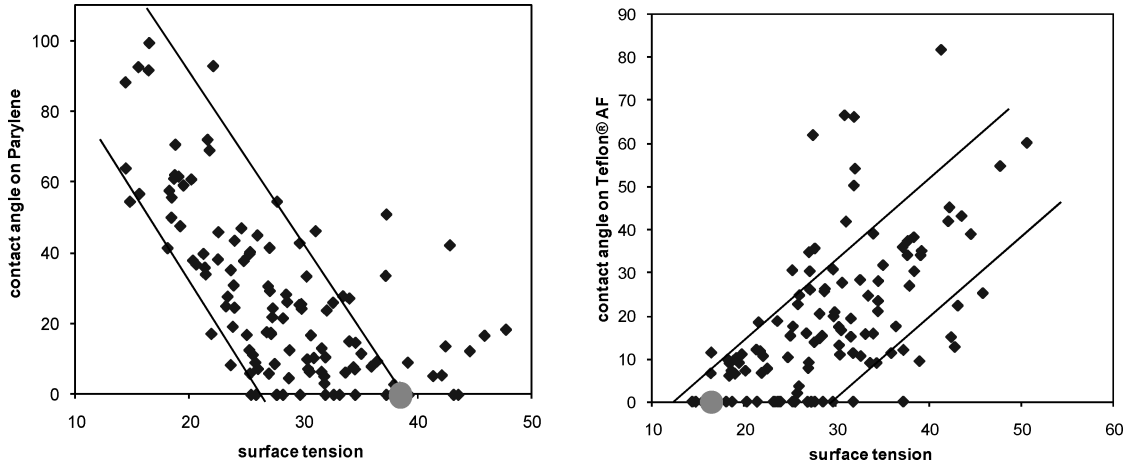

Figure 8. (A) Contact angle from various oil compounds on a parylene C coating, in the conducting fluid described in Table 1, depending on the surface tension of the oil compound. (B) Contact angle from various oil compounds on a Teflon AF coating, in the conducting fluid described in Table 1, depending on the surface tension of the oil compound.

This is well-illustrated in Figure 5, where contact angle has been measured using the same liquids, using parylene substrate having substantially the same dispersive component and variable polar component. These coatings are made in various batches of parylene C; the ones having a polarity above 2 mN/m are aged in the presence of water (typically 12 h at 85 °C in the presence of water) prior to the contact angle measurement, in order to increase the surface polarity. From these results, it appears clearly that, indeed, the polar component from the substrate has a major effect on the resulting two-liquid contact angle.

This is usually true for most two immiscible liquid systems like oil in an aqueous phase: oil is almost a purely dispersive liquid, whereas aqueous fluid is very polar (see Table 2 for the liquids described in Table 1):

The other two optimizations concern the liquid design: the interfacial influence and the nonpolar affinity. The contact angle of two liquids on a surface has been much less studied in the past than wetting properties of a single liquid,[15,16] and it was interesting to develop a tool to predict the behavior of this three-body system.

An equation can be derived from Young's equation with one liquid, taking into account each liquid separately and the two liquids (eq 2).

$$\gamma_S = \gamma_{SW} + \gamma_W \cos\theta_W \quad (7)$$

$$\gamma_S = \gamma_{SO} + \gamma_O \cos\theta_O \quad (8)$$

The three equations are combined to give the Bartell−Osterhof eq 9:[15]

$$\gamma_{OW} \cos\theta_{OW} = \gamma_O \cos\theta_{OS} - \gamma_W \cos\theta_{WS} \quad (9)$$

We developed a graphical representation of the Bartell−Osterhof equation, considering that each term of this equation can be represented as a projection from a trigonometric circle of each surface tension, taking the contact angle of each liquid in air as a coordinate for the surface tension vector of each liquid. According to the Bartell−Osterhof equation, the projection $\gamma_{OW} \cos\theta_{OW}$ is the sum of the two liquid vector projections along the X axis, the coordinate of this vector, i.e., the two liquid contact angle is thus given by the intersection of the projection with a circle of radius equal to the interface tension. This method is represented in Figure 6.

This graphical representation can be advantageously used to visually predict the effect of a change in the surface properties or one of the liquids. Hence, in Figure 7, we represented the effect of lowering the interface tension between the polar liquid and the hydrophobic surface in addition to a decrease in the contact angle from the polar liquid on the hydrophobic surface, which would be expected in such a case. As observed in the graph, this modification of the initial parameters induces an increase in the two liquid contact angle.

It has to be noted that this model is only relevant if contact angles of each individual liquid are >0 when observed on a given substrate, i.e., when none of the liquids are in the total wetting situation. In the latter case, it is also important to take into account the nonpolar affinity to predict the wetting properties, as described previously.

In Figure 8, the contact angles from various nonpolar liquids have been measured with the same polar liquid on a parylene and Teflon AF substrate. The first one is a high surface energy substrate (γ_s = 40 mN/m), whereas the second is a very low surface energy substrate (γ_s = 15 mN/m). The circle corresponds to the substrate surface energy. As observed in graph A, compounds having the lowest contact angle on parylene are statistically those having the highest surface tension whereas those having the lowest contact angle on Teflon AF correspond to the liquids having the lowest surface tension (Figure 8B). A representative list of these compounds is given in Table 3. It is interesting to note that, in the case of a high surface energy coating like parylene, oils that present the lowest contact angle when immersed in the polar solvent like those having the highest surface energy, i.e., the ones that would most likely have the largest contact angle if measured on the same substrate in air. On the contrary, a nonpolar component like a perfluoroalcane that totally spread in air on parylene has the greatest contact angle when measured in the presence of the polar liquid. This wetting paradox also illustrates the nontrivial aspect of the two liquid spreading behavior.

In both graphs, the circle represents the hydrophobic coating surface energy.

(15) Bartell, F. E.; Zuidema, H. H. *J. Am. Chem. Soc.* **1936**, *58*, 1449.
(16) Svitova, T.; Theodoly, O.; Christiano, S.; Hill, R. M.; Radke, C. J. *Langmuir* **2002**, *18*, 6821.
(17) Beach, W. F.; Lee, C.; Bassett, D. R.; Austin, T. M.; Olson, R. *Encycl. Polym. Sci. Eng. 1985−1989* **1989**, *17*, 990.

This result can be simply described by Girifalcos's and Young's equations (eqs 2 and 4) with two liquids and if we consider a liquid and a substrate to be both nonpolar and have substantially the same surface tension and energy ($\gamma_S^d = \gamma_O^d$; $\gamma_S^p = \gamma_O^p \approx 0$). On the basis of eq 4, we can expect an interface tension between a nonpolar liquid and substrate to be close or equal to zero. In that case, Young's equation becomes $\cos\theta_{OW} = (\gamma_{SW} - \gamma_{SO})/\gamma_{OW} \approx \gamma_{SW}/\gamma_{OW}$. As $\gamma_{SW} > \gamma_{SO}$ because oil surface tension is close to the surface energy and the surface is hydrophobic, we obtain $\cos\theta_{OW} > 1$, indicating a total wetting situation.

On the basis of these results, we have been able to obtain an electrowetting system having a very low hysteresis using liquids having very low contact angle, typically below 15° on parylene. As observed in Figure 2, contact angle hysteresis measured by electrowetting is lower than 2°.

The basic requirements to obtain a low contact angle and a low hysteresis system are thus the following:

- Low polarity hydrophobic surfaces, typically surfaces having a polar component measured below 1 mN/m.
- Nonpolar liquids having a surface tension close to the substrate surface energy.
- Preferentially liquids having low interface tension.

Conclusion

Low hysteresis is an important requirement for many electrowetting applications. We present an experimental study of the parameters that lead to low hysteresis devices, from the liquid and the hydrophobic surface points of view.

Our experimental results show that Young's contact angle is a key parameter to achieve low hysteresis electrowetting devices. We point out that surface polarity is also a critical parameter to achieve low hysteresis, and we present some design rule to formulate liquids having a low oil contact angle on a given hydrophobic surface. We also present a graphical method for solving the Bartell−Osterhof equation, a tool to design liquids having low contact angle and consequently low electrowetting hysteresis.

Note Added after ASAP Publication. This article was released ASAP on April 27, 2009. A reference citation that was inadvertently omitted in the Introduction was added. The correct version of the article was posted on May 22, 2009.